



## OPEN ACCESS

## EDITED BY

Giorgio Maria Callovini,  
Azienda Ospedaliera San Giovanni  
Addolorata, Italy

## REVIEWED BY

Felix Mircea Brehar,  
Carol Davila University of Medicine and  
Pharmacy, Romania  
Martin Májovský,  
Charles University, Czechia

## \*CORRESPONDENCE

Tao Lin  
✉ Drlin999gz@163.com  
Da Liu  
✉ 81484153@qq.com

<sup>†</sup>These authors have contributed equally to  
this work and share first authorship

RECEIVED 13 December 2024

ACCEPTED 26 May 2025

PUBLISHED 10 June 2025

## CITATION

Chen Z, Luo W, Lin Y, Deng B, Zhang X,  
Zeng Y, Lin T and Liu D (2025) Diagnostic  
yield of intraoperative frozen sections  
obtained through robot-assisted stereotactic  
biopsy of brain lesions.  
*Front. Neurol.* 16:1544613.  
doi: 10.3389/fneur.2025.1544613

## COPYRIGHT

© 2025 Chen, Luo, Lin, Deng, Zhang, Zeng,  
Lin and Liu. This is an open-access article  
distributed under the terms of the [Creative  
Commons Attribution License \(CC BY\)](https://creativecommons.org/licenses/by/4.0/). The  
use, distribution or reproduction in other  
forums is permitted, provided the original  
author(s) and the copyright owner(s) are  
credited and that the original publication in  
this journal is cited, in accordance with  
accepted academic practice. No use,  
distribution or reproduction is permitted  
which does not comply with these terms.

# Diagnostic yield of intraoperative frozen sections obtained through robot-assisted stereotactic biopsy of brain lesions

Zhijie Chen<sup>1†</sup>, Wangchi Luo<sup>2†</sup>, Yu Lin<sup>3</sup>, Bin Deng<sup>1</sup>, Xubiao Zhang<sup>1</sup>,  
Yongqin Zeng<sup>1</sup>, Tao Lin<sup>1\*</sup> and Da Liu<sup>1\*</sup>

<sup>1</sup>Department of Neurosurgery, Guangdong Sanjiu Brain Hospital, Guangzhou, China, <sup>2</sup>Department of Neurology, The Fourth Affiliated Hospital of Guangzhou Medical University, Guangzhou, China, <sup>3</sup>Department of Laboratory, Guangdong Sanjiu Brain Hospital, Guangzhou, China

**Objective:** To evaluate the diagnostic yield and diagnostic accuracy of intraoperative frozen sections obtained through robot-assisted stereotactic biopsy of brain lesions.

**Methods:** The medical records of 87 patients who underwent 89 robot-assisted stereotactic biopsies of brain lesions at our institution between June 2015 and January 2024 were retrospectively reviewed. All patients were assessed using hematoxylin/eosin (HE) staining of intraoperative frozen sections, and intraoperative immunohistochemical examination when necessary. A final diagnosis derived from integrated diagnostics (neoplastic diseases) or final histopathologic examination (non-neoplastic diseases) was the 'gold standard'. Intraoperative frozen section results were divided into 3 categories: confirmed diagnosis, tentative diagnosis, and misdiagnosis. Subgroup analyses of negative intraoperative frozen section results, tentative diagnoses or misdiagnoses were conducted stratified by lesion size and lesion type.

**Results:** Mean turn-around time for intraoperative frozen sections was  $26 \pm 5.6$  min (range, 20–62 min). 1 (FS-1) to 4 (FS-N) (median, 1) intraoperative frozen sections were evaluated per patient. There was a significant increase in positive results from FS-1 (79.77%;  $n = 71/89$ ) to FS-N (92.13%;  $n = 82/89$ ) ( $p = 0.018$ ). FS-1 results were negative in 18 (20.22%) patients. Among these, FS-N results were positive after adjusting the puncture depth or changing the target in 11 patients. The overall concordance rate of intraoperative frozen section to final diagnosis was 91.1% (confirmed diagnosis,  $n = 73$ ; tentative diagnosis,  $n = 8$ ). Intraoperative immunohistochemistry was performed on the frozen sections of 38 patients (42.7%). Among the patients with negative FS-1 results, tentative diagnoses or misdiagnoses, there were 12, 6 and 7 patients with medium sized lesions, respectively. Eight patients with negative FS-1 results had high-grade glioma.

**Conclusion:** The diagnostic yield of intraoperative frozen sections obtained through robot-assisted stereotactic biopsy of brain lesions is high. If the first frozen section result is negative, additional specimens should be obtained after adjusting the puncture depth or the target. Lesions that are difficult to distinguish morphologically on HE staining may be examined using intraoperative immunohistochemistry. High-grade glioma may be more prone to tentative or misdiagnosis due to heterogeneity of the lesion.

## KEYWORDS

brain tumor, stereotactic biopsy, robotics, frozen section, diagnostic yield

## 1 Introduction

The World Health Organization (WHO) has identified more than 100 types of benign and malignant brain and central nervous system (CNS) lesions that are unique and histologically complex (1). These lesions comprise an estimated 1.9% of all cancers and cause 2.5% of all cancer deaths (2). Brain and CNS lesions are associated with high morbidity and mortality, necessitating accurate diagnosis and timely treatment.

Accurate diagnosis of brain lesions has been facilitated by technological advancements, but the misdiagnosis rate remains high at approximately 30% (3). Stereotactic brain biopsy is a frequently performed, highly efficient, minimally invasive brain surgery that enables precise sampling of pathological brain tissue for histological analysis using a stereotactic needle (4–8). The robotized technique allows the programming of accurate and predefined trajectories, which can be repeated with the same precision, or reprogrammed, minimizing errors that may be made by surgeons (7). Evidence suggests that robot-guided stereotactic techniques are safe and effective for biopsies of brain lesions; however, there is a risk of misdiagnosis or false negative diagnosis due to off-target sampling during the needle puncture procedure.

Intraoperative frozen-section histology can be used to determine the presence of pathological tissue in biopsy specimens (7). Diagnostic yield of stereotactic brain biopsy varies from 72.8 to 100%, but is consistently over 86.7% using intraoperative frozen sections (5, 9–13). Intraoperative frozen section diagnosis is cost-effective and can provide reliable information (14); however, some studies suggest that it can be time-consuming, provides insufficient specimens for a definitive histological interpretation, can increase complications, and requires a well-trained pathologist (15).

Surgeons must strive for the highest diagnostic yield and diagnostic accuracy when treating brain lesions, while minimizing the morbidity and mortality that can be associated with intracranial biopsy (14). To further inform surgeons involved in stereotactic biopsy procedures, this study describes our experience evaluating intraoperative frozen sections obtained through robot-assisted stereotactic biopsy of brain lesions.

## 2 Methods

### 2.1 Data source

The medical records of patients who underwent robot-assisted stereotactic biopsy of brain lesions at our institution between June 2015 and January 2024 were retrospectively reviewed. Preoperatively, patients' physical fitness was assessed using 2016 American Society of Anesthesiologists (ASA) classification criteria, and all patients underwent a preoperative head computed tomography (CT) scan and magnetic resonance imaging (MRI) (T1-weighted, T2-weighted, T2-weighted fluid attenuated inversion recovery [FLAIR], contrast-enhanced), with some patients also undergoing positron emission tomography

(PET)-CT, MR spectroscopy (MRS), arterial spin labeling (ASL), and if necessary, lumbar puncture for examination of cerebrospinal fluid.

Inclusion criteria were: (1) brain lesion that was difficult to diagnose with non-invasive imaging; (2) lesion located next to sensitive structures, such that open surgery was associated with an extremely high risk of loss of function; (3) diagnosis on imaging required pathological confirmation before radiotherapy or chemotherapy (e.g., germ cell tumor, lymphoma); (4) highly malignant lesion or postoperative recurrence of a benign tumor with worsening symptoms, with family refusing repeat craniotomy; (5) need to differentiate between tumor progression and radiation necrosis after comprehensive treatment of an intracranial tumor; and (6) patient and family provided consent for robot-assisted stereotactic biopsy. Exclusion criteria were: (1) ASA class  $\geq$  V; (2) contraindication to surgery due to coagulation dysfunction; (3) imaging suggestive of brain herniation; or (4) patient and family refused robot-assisted stereotactic biopsy.

### 2.2 Surgical procedure and frozen section

Preoperatively, multidisciplinary discussions involved the Departments of Neurosurgery, Neurology, Radiology, Oncology, and Pathology. Targeted biopsies were performed along trajectories that avoided functional areas of the brain. The biopsy procedures were assisted by the SINO robot (Sinovation Medical, China). After biopsy, normal saline solution was dripped from the end of the puncture needle to promote hemostasis.

In this study, robot-assisted stereotactic biopsies of brain lesions were performed by a team of experienced neurosurgeons from our hospital's Department of Neurosurgery. A total of four neurosurgeons participated in the 89 robot-assisted stereotactic biopsy procedures. All these surgeons had undergone specialized training to ensure the precision and consistency of the surgical procedures.

The nature and color of stereotactic puncture specimens were observed. 1–2 samples (0.1 cm  $\times$  1 cm) with an abnormal appearance (e.g., gelatinous) were sent for intraoperative frozen section examination, and 2–4 samples were retained for final histopathologic examination and molecular testing. For neoplastic diseases, if the final histopathologic examination could not make a definite diagnosis, supplementary genetic testing using fluorescence *in situ* hybridization (FISH), gene rearrangement, and polymerase chain reaction (PCR) was performed.

Intraoperative frozen sections were cut sequentially at 0.2 cm intervals using a LEICA CM1950 cryostat (Leica, Germany), with the temperature set at  $-19$  to  $-20^{\circ}\text{C}$ , and a slice thickness of 4  $\mu\text{m}$ . The first intraoperative frozen section was designated FS-1, and subsequent intraoperative frozen sections were designated FS-N ( $N = 2, 3$  or 4). 2–3 slices per tissue were examined under a light microscope after hematoxylin/eosin (HE) staining to observe specimen morphology and make a preliminary diagnosis. If intraoperative diagnosis was difficult on an HE stained frozen section, immunohistochemistry was performed. Remaining slices were paraffin embedded for final

histopathologic examination. This ensured consistency between frozen section analysis and final permanent pathology.

## 2.3 Definitions

FS-1 represents the first intraoperative frozen section, while FS-N represents subsequent intraoperative frozen sections, where  $N$  is 2, 3, or 4, depending on the total number of frozen sections evaluated for each patient. At least one frozen section (FS-1) was evaluated for each patient, with a maximum of four frozen sections (FS-N,  $N = 2, 3, \text{ or } 4$ ) evaluated. If the result of FS-1 was negative, the puncture depth was adjusted or the target point was changed according to the location and characteristics of the brain lesion to obtain additional sections (FS-2 to FS-4). This process was based on the professional judgment of the surgeon according to the characteristics of the brain lesion and results from the preliminary section.

## 2.4 Diagnostic standard

Intraoperative frozen sections were evaluated against integrated diagnoses (incorporating molecular parameters) as the gold standard. Neoplastic lesions were classified according to the 2016 WHO Classification of CNS Tumors (16), with consideration of the 2021 WHO Classification updates (17) where relevant.

Intraoperative frozen section results were divided into 3 categories, as previously described (18, 19):

- (1) Confirmed diagnosis: intraoperative diagnosis matched the integrated final diagnosis in both tumor identification and grading. For gliomas, this included correct identification of molecular features when available (IDH status, 1p/19q codeletion), recognizing the 2021 WHO Classification's simplified categories for IDH-mutant gliomas and refined molecular criteria for IDH-wildtype glioblastoma. For lymphomas, this required accurate identification of lymphoid proliferation with supporting morphological and immunohistochemical evidence.
- (2) Tentative diagnosis: correct identification of lesion nature but incomplete classification or grading. This included cases where definitive diagnosis required additional molecular testing unavailable intraoperatively, particularly relevant as the 2021 WHO Classification emphasizes molecular parameters for definitive diagnosis.
- (3) Misdiagnosis: false positive/negative results or incorrect tumor identification.

Both confirmed and tentative diagnoses were considered correct. Multiple biopsies with identical results were combined, and when both high-grade and low-grade components were present, the highest grade was reported.

## 2.5 Statistical analyses

Analyses were performed with SPSS v26.0 using descriptive statistics. Data are reported as means ( $\pm$  standard deviations) or

ranges for quantitative variables, and as absolute numbers and/or percentages for categorical variables.

## 3 Results

### 3.1 Patients

This study included 87 patients (56 males and 31 females), with a mean age of  $39.1 \pm 21.6$  years (range, 3.2–76 years). 73 patients were ASA class I-II, 12 patients were ASA class III, and 2 patients were ASA class IV. All patients had brain lesions, 56 patients had multiple or diffuse lesions (involving multiple brain lobes) and 31 patients had single lesions. Mean diameter of the lesions was  $5.12 \pm 2.90$  cm (range, 0.8 ~ 12.5 cm). Two patients had negative biopsy results and underwent a second robot-assisted stereotactic biopsy; therefore, there were a total of 89 biopsy procedures of 97 target lesions. Lesions were categorized into three types in accordance with their longest diameters: small ( $< 2$  cm), medium (2–5 cm), and giant ( $> 5$  cm). Patients' demographic and clinical characteristics and characteristics of the lesions are summarized in Table 1.

TABLE 1 Patients' demographic and clinical characteristics and characteristics of the lesions.

| Characteristic (N = 87)     | Value                       | Characteristic (N = 89)       | Value |
|-----------------------------|-----------------------------|-------------------------------|-------|
| Age (years)                 |                             | Biopsy region                 |       |
| Mean $\pm$ SD               | 39.1 $\pm$ 21.6             | Frontal lobe                  | 22    |
| Range                       | 3.2–76                      | Temporal lobe                 | 9     |
| Gender                      |                             | Parietal lobe                 | 2     |
| Female                      | 40                          | Occipital lobe                | 3     |
| Lesion size (cm)            | 5.12 + 2.99 cm<br>(1–12 cm) | Thalamus and/or basal ganglia | 28    |
| Lesion size                 |                             | Midbrain                      | 7     |
| Small ( $\leq 2$ cm)        | 6                           | Pons                          | 13    |
| Medium (2–5 cm)             | 45                          | Medulla oblongata             | 0     |
| Giant ( $\geq 5$ cm)        | 36                          | Cerebellum                    | 2     |
| Sides involved              |                             | Corpus callosum               | 3     |
| Right                       | 24                          | Other regions*                | 2     |
| Left                        | 26                          | Biopsy side                   |       |
| Bilateral                   | 37                          | Left                          | 30    |
| Lesion presentation         |                             | Right                         | 54    |
| Multiple or diffuse lesions | 56                          | Bilateral                     | 5     |
| Single                      | 31                          |                               |       |
| Brain regions involved      |                             |                               |       |
| Limited to 1 region         | 16                          |                               |       |
| 2–3 regions                 | 31                          |                               |       |
| > 3 regions                 | 30                          |                               |       |

\*Other regions include optic chiasm, optic tract, fourth ventricle, septum pellucidum, lateral ventricles, etc.

### 3.2 Diagnostic yield of the stereotactic biopsy procedure

Intraoperative frozen section biopsy results are summarized in Table 2, Figures 1 and 2. Mean turn-around time for intraoperative frozen sections was 26 ± 5.6 min (range, 20–62 min). 1 to 4 (median, 1) intraoperative frozen sections were evaluated per patient.

The overall concordance rate of intraoperative frozen section to final diagnosis was 91.1% (confirmed diagnosis, *n* = 73; tentative diagnosis, *n* = 8). 8 patients were misdiagnosed on intraoperative frozen section, including 5 cases with negative intraoperative frozen section results. Intraoperative immunohistochemistry was performed on the frozen sections of 38 patients (42.7%) to clarify the nature of their lesions.

There was a significant increase in positive results from FS-1 (79.77%; *n* = 71/89) to FS-N (92.13%; *n* = 82/89) (*p* = 0.018, Table 2). FS-1 results were negative in 18 (20.22%) patients. Among these, FS-N results were positive after adjusting the puncture depth or changing

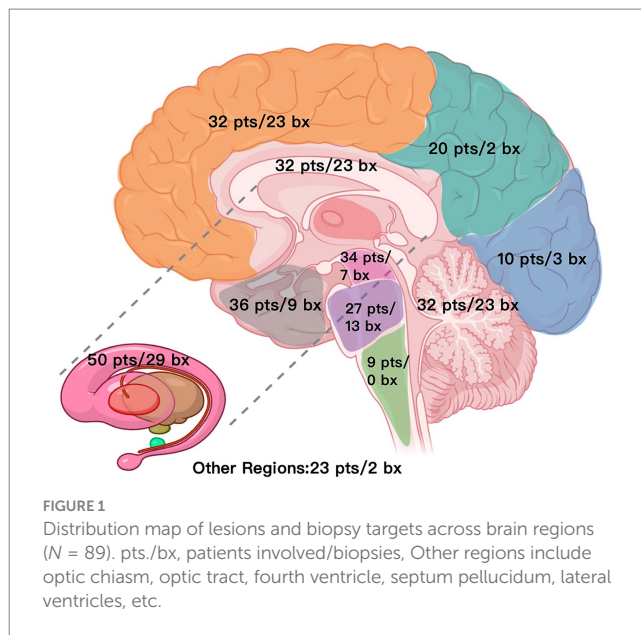


FIGURE 1 Distribution map of lesions and biopsy targets across brain regions (N = 89). pts./bx, patients involved/biopsies, Other regions include optic chiasm, optic tract, fourth ventricle, septum pellucidum, lateral ventricles, etc.

TABLE 2 Intraoperative frozen section biopsy results (N = 89).

| Variable                                  | Case no. | Percentage | <i>p</i> -value   |
|---|----------|------------|-------------------|
| DY of first FS                            | 71       | 79.77%     | <i>P</i> = 0.018* |
| DY of FS                                  | 82       | 92.13%     |                   |
| DY of final diagnosis                     | 85       | 96.55%     | <i>p</i> = 0.29#  |
| Accuracy of FS (N = 89)                   | 73       | 82.02%     |                   |
| Concordance of FS (N = 89)                | 81       | 91.01%     |                   |
| Concordance of radiology ( <i>n</i> = 87) | 69       | 79.31%     |                   |
| IHC applied in FS                         | 38       | 42.69%     | /                 |
| Diagnosis results                         |          |            |                   |
| Confirmed diagnosis                       | 74       | 83.14%     | /                 |
| Tentative diagnosis                       | 7        | 7.87%      | /                 |
| Misdiagnosis                              | 8        | 8.99%      | /                 |
| False negative FS                         | 6        | 6.7%       | /                 |
| False positive FS                         | 2        | 2.2%       | /                 |
| Diagnosis ( <i>n</i> = 87)                |          |            |                   |
| Grade I-II glioma                         | 9        | 10.3%      | /                 |
| Grade III-IV glioma                       | 43       | 49.42%     | /                 |
| Lymphoma                                  | 26       | 29.89%     | /                 |
| Germ cell tumor                           | 4        | 4.6%       | /                 |
| Inflammation                              | 3        | 3.45%      | /                 |
| Brain tissue                              | 1        | 1.15%      | /                 |
| Gliosis                                   | 1        | 1.15%      | /                 |

\*Comparison of first frozen section diagnostic yield and final frozen section diagnostic yield.

#Comparison of frozen section diagnostic concordance rate and radiology diagnostic concordance rate.

DY, diagnostic yield; IHC, immunohistochemistry; FS, frozen section.

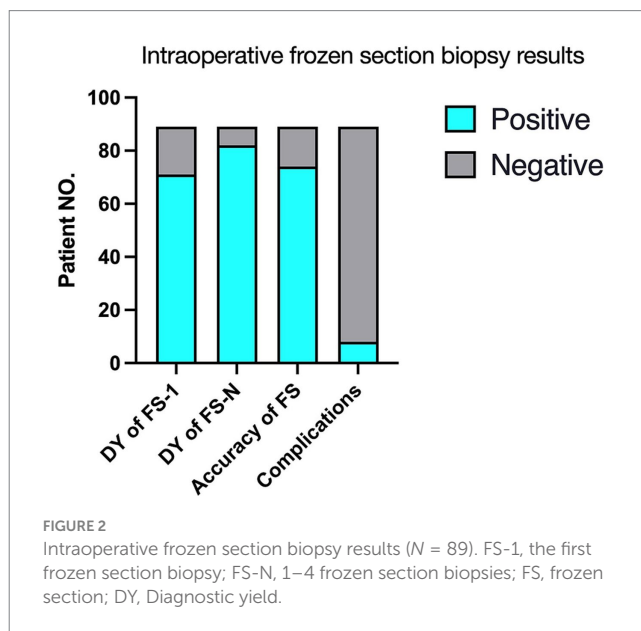


FIGURE 2 Intraoperative frozen section biopsy results (N = 89). FS-1, the first frozen section biopsy; FS-N, 1–4 frozen section biopsies; FS, frozen section; DY, Diagnostic yield.

the target in 11 patients or had the same negative interpretation in the other 7 patients.

Six patients had postoperative hematoma in the surgical area, including 5 patients with asymptomatic bleeding. One patient had severe delayed cerebral hemorrhage, which resulted in death. One patient with diffuse glioma experienced a postoperative seizure, which led to a sharp rise in intracranial pressure along with diffuse brain swelling, cerebral herniation, and death. Details are shown in Table 3. No other patients had surgery-related neurological dysfunction or intracranial infection.

Subgroup analyses of negative FS-1 results, tentative diagnoses or misdiagnoses were conducted stratified by lesion size and lesion type. 18 patients had negative FS-1 results, including 12 patients with medium sized lesions, 5 patients with giant lesions, 8 patients with high-grade glioma, 5 patients with low-grade glioma and 3 patients with lymphoma. Of these, 3 patients each with medium and giant

TABLE 3 Complications of robot-assisted stereotactic biopsy.

| Variable                      | Case no. | Percentage |
|-------------------------------|----------|------------|
| <b>Complications (n = 89)</b> |          |            |
| Small bleed                   | 6        | 6.74%      |
| Symptomatic bleeding          | 2        | 2.22%      |
| Inflammation                  | 1        | 1.11%      |
| Pneumonia                     | 2        | 2.22%      |
| Dead                          | 2        | 2.22%      |
| Epilepsy                      | 1        | 1.11%      |

lesions, and 4 patients with high-grade glioma had the same negative interpretation on FS-N results. All the patients with lymphoma had positive FS-N results. Eight patients had a tentative diagnosis, including 6 patients with medium sized lesions, 2 patients with giant lesions, and 5 patients with high-grade glioma. Eight patients were misdiagnosed, including 7 patients with medium sized lesions, 1 patient with a giant lesion, and 5 patients with high-grade glioma (Table 4).

### 3.3 Pathological diagnosis

Among the 87 patients, final diagnoses included glioma ( $n = 52$ ; WHO grade I-II,  $n = 9$ ; WHO grade III-IV,  $n = 43$ ), lymphoma ( $n = 26$ ), germ cell tumor ( $n = 4$ ), inflammation ( $n = 3$ ), gliosis ( $n = 1$ ), and normal brain tissue ( $n = 1$ ). For one patient, FS-1-4 results were reported as negative, a qualitative diagnosis was difficult on routine pathology, and the patient was ultimately diagnosed with T-cell lymphoma through genetic testing. One patient with recurrent low-grade glioma underwent biopsy of two targets, and the results were high-grade glioma and low-grade glioma. The patient was diagnosed as high-grade glioma.

Ten patients with lymphoma had received steroid treatment before the biopsy procedure (range, 2 weeks - 6 months). Among these, one patient was diagnosed with inflammation on intraoperative frozen section, but the final diagnosis was lymphoma. One patient was negative on FS-1 and positive on FS-N, while the other patients were all positive on FS-1.

## 4 Discussion

This study evaluated the diagnostic yield and diagnostic accuracy of intraoperative frozen sections obtained through robot-assisted stereotactic biopsy of brain lesions. Findings showed mean turn-around time for intraoperative frozen sections was  $26 \pm 5.6$  min (range, 20–62 min). The diagnostic yield of intraoperative frozen sections was 91.01%. In accordance with previous studies (6, 20, 21), the diagnostic yield was increased by examining multiple tissue specimens, after the target or puncture depth had been adjusted (79.77% for FS-1 increasing to 92.13% for FS-N) (6, 20, 21). The diagnostic yield of preoperative imaging (MR and/or CT) was 79.31% ( $n = 69/87$ ), with potential for misdiagnosis if treatment decision-making had been based on preoperative

imaging alone. FS-1 results were negative in 18 (20.22%) patients; of these, FS-2 results were positive in 11 patients. This may be because many lesions were located at functional areas (e.g., brainstem, thalamus, basal ganglia) and the characteristics of FS-1 were only representative of the lesion periphery. The remaining 7 patients were still negative on FS-3 or FS-4. Some of these negative results were false negatives, as the diagnostic yield of the 'gold standard' approach of integrated diagnostics (neoplastic diseases) or histopathological examination (non-neoplastic diseases) was 96.63% ( $n = 86/89$ ). Lesions that were difficult to distinguish morphologically on HE staining were examined immediately using intraoperative immunohistochemistry, adding to the turn-around time for intraoperative frozen sections. The 38 patients that underwent intraoperative immunohistochemistry included 21 of 26 (80.77%) patients with lymphoma, 13 patients with high-grade glioma, 3 patients with low-grade glioma, and 1 patient with germ cell tumor. Subgroup analyses showed that most patients with negative FS-1 results, tentative diagnosis or misdiagnosis, had medium sized lesions, and that high-grade glioma was prone to tentative and misdiagnosis, possibly due to the heterogeneity of the lesion (22, 23). These results imply that intraoperative frozen section obtained through robot-assisted stereotactic biopsy has clinical utility for determining the nature of brain lesions.

Currently, intraoperative frozen sections are not routinely obtained through stereotactic brain biopsy. Factors limiting widespread adoption of this approach include the small amount of biopsy tissue, prolonged operative-time, the relatively high technical requirements for frozen sections, the potential for false negative or false positive diagnoses due to errors in sampling and processing and varied experience of pathologists, and the high incidence of complications such as cerebral hemorrhage and dysfunction (15, 24–26). A search of the literature published in English since 1995 on the PubMed Medline database using the keyword "stereotactic brain biopsy," showed only 11 studies reported on the use of intraoperative frozen sections (5, 9, 10, 12, 14, 21, 27–30) (Table 5). In these studies, the diagnostic yield ranged from 70.1–98.2%, and the diagnostic yield of final pathology was 87.6–98.7% (5, 9, 10, 12, 14, 21, 27–30). One study of MRI-based robot-assisted stereotactic biopsy in which the majority of patients had an intraoperative pathologic diagnosis with frozen sections showed that complication rates did not increase with the number of biopsy sites and complications were not associated with the number of biopsy samples (5).

Several factors can lead to false negatives or misdiagnosis on intraoperative frozen sections. In the current study, false negatives or misdiagnosis occurred as (1) the scalp incision and trephination through which the biopsy needle was advanced did not align with the lesion; (2) the surgeon misinterpreted preoperative imaging and selected an atypical area as the target site; (3) the surgeon chose a target that was representative of the lesion periphery to avoid functional areas; and/or (4) improper robot operation. In our early cases, we overlooked a critical technical detail regarding the Sedan side-cutting biopsy needle. This needle (198 mm working length) has a 2 mm blind tip and a 10 mm side-cutting window. To align the window's center with the target, we should have set the robotic working distance to 190–192 mm rather than the full 198 mm. This miscalculation likely contributed to some false-negative results in our initial series of biopsies.

TABLE 4 Subgroup analyses of intraoperative FS-1 results reported as negative, tentative diagnoses or misdiagnoses.

| Variable             | Negative on FS-1<br>(N = 18) | Negative on FS-N<br>(N = 7) | Tentative diagnosis<br>(N = 8) | Misdiagnosis<br>(N = 8) |
|----------------------|------------------------------|-----------------------------|--------------------------------|-------------------------|
| <b>Lesion size</b>   |                              |                             |                                |                         |
| Small ( $\leq 2$ cm) | 1                            | 1                           | 0                              | 0                       |
| Medium (2–5 cm)      | 12                           | 3                           | 6                              | 7                       |
| Giant ( $\geq 5$ cm) | 5                            | 3                           | 2                              | 1                       |
| <b>Lesion types</b>  |                              |                             |                                |                         |
| Grade I–II glioma    | 5                            | 1                           | 2                              | 0                       |
| Grade III–IV glioma  | 8                            | 4                           | 5                              | 5                       |
| Lymphoma             | 3                            | 0                           | 1                              | 2                       |
| Germ cell tumor      | 1                            | 1                           | 0                              | 1                       |
| Inflammation         | 0                            | 0                           | 0                              | 0                       |
| Brain tissue         | 1                            | 1                           | 0                              | 0                       |
| Gliosis              | 0                            | 0                           | 0                              | 0                       |

TABLE 5 Studies that have applied frozen sections in stereotactic biopsy of brain lesions in the past 30 years.

| No. | Reference                    | FS applied | DY of FS | DY of final pathology | Concordance rate of FS | Surgical technique | Surgical equipment | Number of biopsies |
|-----|------------------------------|------------|----------|-----------------------|------------------------|--------------------|--------------------|--------------------|
| 1   | Current study                | All cases  | 96.65%   | 96.65%                | 91.3%                  | Robot              | ROSA, SINO         | 89                 |
| 2   | Hayden et al. (12)           | All cases  | 78%      | 86.7%                 | 75%                    | Frame              | BRW, CRW           | 75                 |
| 3   | Brainard et al. (21)         | All cases  | 84.04%   | 96.27%                | 88.83%                 | Frame              | BRW, CRW, COMPASS  | 188                |
| 4   | Kim et al. (28)              | 92%        | 90.1%    | 91.7%                 | 79%                    | Frame              | Riechert-Mundinger | 308                |
| 5   | Gralla et al. (27)           | All cases  | 98.2%    | 94.8%                 | 96.5%                  | Frameless          | Stealth Treon      | 57                 |
| 6   | Woodworth et al. (9)         | All cases  | /        | 91%                   | 70%                    | Frame              | Leksell            | 160                |
|     |                              |            | /        | 89%                   | 78%                    | Frameless          | FreeGuide          | 110                |
| 7   | Dammers et al. (14)          | 8.9%       | /        | 98.2%                 | /                      | Frameless          | Stealth Treon      | 164                |
| 8   | Mader et al. (30)            | 51.3%      | 75.4%    | 92.4%                 | 78.7%                  | Frame              | Leksell            | 110                |
| 9   | Taweessomboonyat et al. (10) | 76%        | 70.1%    | 87.6%                 | 81%                    | Frameless          | VarioGuide         | 85                 |
| 10  | Legnani et al. (29)          | Some cases | /        | 97.4%                 | /                      | Micro-robot        | iSYS1              | 39                 |
| 11  | Shofty et al. (32)           | 90.9%      | /        | 96.8%                 | /                      | Frameless          | VarioGuide         | 376                |
| 12  | Zanello et al. (16)          | Most cases | 97.2%    | 98.7%                 | /                      | Robot              | Neuromate          | 324                |
| 13  | Majovsky et al. (36)         | 37.6%      | 66.67%   | 66.67%                | 59.09%                 | Frame, Frameless   | CRW, VarioGuide    | 125                |

Misinterpretation of intraoperative frozen sections can also impact the accuracy of diagnosis (31). To avoid false negatives or misdiagnosis, we recommend: (1) retrieving a specimen from the center of a small or medium sized lesion, but avoiding the central necrotic area for large glioblastoma (32, 33); (2) ensuring the specimen is representative of a brain lesion, with a fish-like appearance in contrast to the milky white appearance of healthy brain tissue; (3) obtaining several specimens by rotating the needle in different directions or varying the depth slightly; and (4) diagnosing intraoperative frozen sections jointly by multiple experienced pathologists.

Intraoperative cytological methods (cytology smear and touch imprint) are also used in stereotactic biopsy to assist in

determining the nature of CNS lesions (12). Applying both cytological methods and frozen sections may improve intraoperative diagnostic accuracy. In one study, touch imprint, cytology smear, and frozen sections had a diagnostic accuracy of 78.4, 89.2, and 75.7%, respectively, and an overall diagnostic accuracy of 96% for CNS lesions (34). In another study, frozen sections and cytology smear had a diagnostic accuracy of 84.6 and 76.9%, respectively and an overall diagnostic yield of 100% for glioma (31). Intraoperative cytology smear may provide a qualitative intraoperative diagnosis in over 25% of cases where frozen sections yield a diagnosis of “equivocal brain tumor” (19). Notably, frozen sections are generally considered superior to

cytological methods for intraoperative diagnosis. Frozen sections can present tissue structure characteristics more clearly, providing certain advantages in determining tumor type and boundaries (35). When diagnosis using frozen sections during stereotactic biopsy is difficult, cytological methods may serve as an alternative.

This study was associated with several limitations. First, the retrospective design may have led to information and selection biases. Second, the sample size from a single center limited the generalizability of the findings and statistical power. Third, intraoperative frozen section assessments are subjective and may vary between pathologists, potentially affecting outcomes.

## 5 Conclusion

This study shows the diagnostic yield of intraoperative frozen sections obtained through robot-assisted stereotactic biopsy of brain lesions is high. When initial results are negative, additional specimens should be obtained by adjusting either puncture depth or target location. Lesions that are difficult to distinguish morphologically on HE staining may be examined using intraoperative immunohistochemistry, although this will increase operative time. High grade glioma may be more prone to tentative or misdiagnosis due to heterogeneity of the lesion.

## Data availability statement

The raw data supporting the conclusions of this article will be made available by the authors, without undue reservation.

## Ethics statement

The studies involving humans were approved by the Ethics Committee of the Guangdong Sanjiu Brain Hospital (No: 2022-010-030). The studies were conducted in accordance with the local legislation and institutional requirements. The participants provided their written informed consent to participate in this study.

## References

- Ostrom QT, Francis SS, Barnholtz-Sloan JS. Epidemiology of brain and other CNS tumors. *Curr Neurol Neurosci Rep.* (2021) 21:68. doi: 10.1007/s11910-021-01152-9
- Ferlay J, Colombet M, Bray F. Cancer incidence in five continents, CI5plus: IARC CancerBase No. 9. Lyon, France: International Agency for Research on Cancer (2018).
- Cheng G, Yu X, Zhao H, Cao W, Li H, Li Q, et al. Complications of stereotactic biopsy of lesions in the Sellar region, pineal gland, and brainstem: a retrospective, single-center study. *Medicine.* (2020) 99:e18572. doi: 10.1097/MD.00000000000018572
- Yasin H, Hoff HJ, Blümcke I, Simon M. Experience with 102 frameless stereotactic biopsies using the NeuroMate robotic device. *World Neurosurg.* (2019) 123:e450–6. doi: 10.1016/j.wneu.2018.11.187
- Zanello M, Roux A, Senova S, Peeters S, Edjlali M, Tauziède-Espariat A, et al. Robot-assisted stereotactic biopsies in 377 consecutive adult patients with Supratentorial diffuse gliomas: diagnostic yield, safety, and postoperative outcomes. *World Neurosurg.* (2021) 148:e301–13. doi: 10.1016/j.wneu.2020.12.127
- Wu S, Wang J, Gao P, Liu W, Hu F, Jiang W, et al. A comparison of the efficacy, safety, and duration of frame-based and Remebot robot-assisted frameless stereotactic biopsy. *Br J Neurosurg.* (2021) 35:319–23. doi: 10.1080/02688697.2020.1812519
- Bex A, Mathon B. Advances, technological innovations, and future prospects in stereotactic brain biopsies. *Neurosurg Rev.* (2022) 46:5. doi: 10.1007/s10143-022-01918-w
- Feng Y, Yaming W, Yongzhi S, Penghu W, Hong W, Xiaotong F, et al. Novel application of robot-guided stereotactic technique on biopsy diagnosis of intracranial lesions. *Front Neurol.* (2023) 14:1173776. doi: 10.3389/fneur.2023.1173776
- Woodworth GF, McGirt MJ, Samdani A, Garonzik I, Olivi A, W JD. Frameless image-guided stereotactic brain biopsy procedure: diagnostic yield, surgical morbidity, and comparison with the frame-based technique. *J Neurosurg.* (2006) 104:233–7. doi: 10.3171/jns.2006.104.2.233
- Taweesomboonyat C, Tunthanathip T, Sae-Heng S, Oearsakul T. Diagnostic yield and complication of frameless stereotactic brain biopsy. *J Neurosci Rural Pract.* (2019) 10:78–84. doi: 10.4103/jnrp.jnrp\_166\_18
- Khatib S, Spliet W, Woerdeman PA. Frameless image-guided stereotactic brain biopsies: emphasis on diagnostic yield. *Acta Neurochir.* (2014) 156:1441–50. doi: 10.1007/s00701-014-2145-2
- Hayden R, Cajulis RS, Frias-Hidvegi D, Brody BA, Yu G, Levy R. Intraoperative diagnostic techniques for stereotactic brain biopsy: cytology versus frozen-section histopathology. *Stereotact Funct Neurosurg.* (1995) 65:187–93. doi: 10.1159/000098693

## Author contributions

ZC: Supervision, Writing – original draft. WL: Project administration, Writing – original draft. YL: Data curation, Writing – review & editing. BD: Data curation, Writing – review & editing. XZ: Formal analysis, Writing – review & editing. YZ: Writing – review & editing. TL: Conceptualization, Writing – review & editing. DL: Conceptualization, Writing – review & editing.

## Funding

The author(s) declare that financial support was received for the research and/or publication of this article. This work was supported by Medical Scientific Research Foundation of Guangdong Province, China (Nos: A2024464 and B2023418) and the Guangzhou Medical University Scientific Research Capacity Enhancement Project (No: 2023KYQB01PT).

## Conflict of interest

The authors declare that the research was conducted in the absence of any commercial or financial relationships that could be construed as a potential conflict of interest.

## Generative AI statement

The authors declare that no Gen AI was used in the creation of this manuscript.

## Publisher's note

All claims expressed in this article are solely those of the authors and do not necessarily represent those of their affiliated organizations, or those of the publisher, the editors and the reviewers. Any product that may be evaluated in this article, or claim that may be made by its manufacturer, is not guaranteed or endorsed by the publisher.

13. Carai A, Mastronuzzi A, De Benedictis A, Messina R, Cacchione A, Miele E, et al. Robot-assisted stereotactic biopsy of diffuse intrinsic pontine glioma: a single-center experience. *World Neurosurg.* (2017) 101:584–8. doi: 10.1016/j.wneu.2017.02.088
14. Dammers R, Schouten JW, Haitsma IK, Vincent AJ, Kros JM, Dirven CM. Towards improving the safety and diagnostic yield of stereotactic biopsy in a single Centre. *Acta Neurochir.* (2010) 152:1915–21. doi: 10.1007/s00701-010-0752-0
15. Shooman D, Belli A, Grundy PL. Image-guided frameless stereotactic biopsy without intraoperative neuropathological examination. *J Neurosurg.* (2010) 113:170–8. doi: 10.3171/2009.12.JNS09573
16. Louis D, Ohgaki H, Wiestler O, Cavenee W. World Health Organization histological classification of tumours of the central nervous system 2016. France: International Agency for Research on Cancer (2016).
17. Louis DN, Perry A, Wesseling P, Brat DJ, Cree IA, Figarella-Branger D, et al. The 2021 WHO classification of tumors of the central nervous system: a summary. *Neuro-Oncology.* (2021) 23:1231–51. doi: 10.1093/neuonc/noab106
18. Tilgner J, Herr M, Ostertag C, Volk B. Validation of intraoperative diagnoses using smear preparations from stereotactic brain biopsies: intraoperative versus final diagnosis—influence of clinical factors. *Neurosurgery.* (2005) 56:257–65. doi: 10.1227/01.neu.0000148899.39020.87
19. Fujita H, Tajiri T, Machida T, Nomura N, Toguchi S, Itoh H, et al. Intraoperative squash cytology provides a qualitative intraoperative diagnosis for cases in which frozen section yields a diagnosis of equivocal brain tumour. *Cytopathology.* (2020) 31:106–14. doi: 10.1111/cyt.12798
20. Dammers R, Haitsma IK, Schouten JW, Kros JM, Avezaat CJ, Vincent AJ. Safety and efficacy of frameless and frame-based intracranial biopsy techniques. *Acta Neurochir.* (2008) 150:23–9. doi: 10.1007/s00701-007-1473-x
21. Brainard JA, Prayson RA, Barnett GH. Frozen section evaluation of stereotactic brain biopsies: diagnostic yield at the stereotactic target position in 188 cases. *Arch Pathol Lab Med.* (1997) 121:481–4.
22. Hoffman LM, Colditz N, Baugh J, Chaney B, Hoffmann M, Lane A, et al. Clinical, radiologic, pathologic, and molecular characteristics of long-term survivors of diffuse intrinsic pontine glioma (DIPG): a collaborative report from the international and European Society for Pediatric Oncology DIPG registries. *J Clin Oncol.* (2018) 36:1963–72. doi: 10.1200/jco.2017.75.9308
23. Nikbakht H, Panditharatna E, Mikael LG, Li R, Gayden T, Osmond M, et al. Spatial and temporal homogeneity of driver mutations in diffuse intrinsic pontine glioma. *Nat Commun.* (2016) 7:11185. doi: 10.1038/ncomms11185
24. Goel D, Sundaram C, Paul TR, Uppin SG, Prayaga AK, Panigrahi MK, et al. Intraoperative cytology (squash smear) in neurosurgical practice - pitfalls in diagnosis experience based on 3057 samples from a single institution. *Cytopathology.* (2007) 18:300–8. doi: 10.1111/j.1365-2303.2007.00484.x
25. Zhou Y, Qi T, Yang Y, Li Z, Hou Z, Zhao X, et al. Effect of different staining methods on brain Cryosections. *ACS Chem Neurosci.* (2024) 15:2243–52. doi: 10.1021/acchemneuro.4c00069
26. Laakman JM, Chen SJ, Lake KS, Blau JL, Rajan DA, Samuelson MI, et al. Frozen section quality assurance. *Am J Clin Pathol.* (2021) 156:461–70. doi: 10.1093/ajcp/aqaa259
27. Gralla J, Nimsky C, Buchfelder M, Fahlbusch R, Ganslandt O. Frameless stereotactic brain biopsy procedures using the Stealth Station: indications, accuracy and results. *Zentralbl Neurochir.* (2003) 64:166–70. doi: 10.1055/s-2003-44620
28. Kim JE, Kim DG, Paek SH, Jung HW. Stereotactic biopsy for intracranial lesions: reliability and its impact on the planning of treatment. *Acta Neurochir.* (2003) 145:547–55. doi: 10.1007/s00701-003-0048-8
29. Legnani FG, Franzini A, Mattei L, Saladino A, Casali C, Prada F, et al. Image-guided biopsy of intracranial lesions with a small robotic device (Isys1): a prospective, exploratory pilot study. *Oper Neurosurg.* (2019) 17:403–12. doi: 10.1093/ons/opy411
30. Mader MM, Rotermund R, Martens T, Westphal M, Matschke J, Abboud T. The role of frameless stereotactic biopsy in contemporary neuro-oncology: molecular specifications and diagnostic yield in biopsied glioma patients. *J Neuro-Oncol.* (2019) 141:183–94. doi: 10.1007/s11060-018-03024-8
31. Plesec TP, Prayson RA. Frozen section discrepancy in the evaluation of central nervous system tumors. *Arch Pathol Lab Med.* (2007) 131:1532–40. doi: 10.5858/2007-131-1532-fsdtte
32. Shofty B, Richetta C, Haim O, Kashanian A, Gurevich A, Grossman R. 5-ala-assisted stereotactic brain tumor biopsy improve diagnostic yield. *Eur J Surg Oncol.* (2019) 45:2375–8. doi: 10.1016/j.ejso.2019.07.001
33. Hu Y, Cai P, Zhang H, Adilijiang A, Peng J, Li Y, et al. A Comparison between frame-based and robot-assisted in stereotactic biopsy. *Front Neurol.* (2022) 13:928070. doi: 10.3389/fneur.2022.928070
34. Nanarng V, Jacob S, Mahapatra D, Mathew JE. Intraoperative diagnosis of central nervous system lesions: comparison of squash smear, touch imprint, and frozen section. *J Cytol.* (2015) 32:153–8. doi: 10.4103/0970-9371.168835
35. Ferreira MP, Ferreira NP, Pereira Filho Ade A, Pereira Filho Gde A, Franciscatto AC. Stereotactic computed tomography-guided brain biopsy: diagnostic yield based on a series of 170 patients. *Surg Neurol.* (2006) 27-1:32. doi: 10.1016/j.surneu.2005.11.036
36. Majovsky M, Moravec T, Komarc M, Soukup J, Sedlak V, Balasubramaniam N, et al. Surgical results in patients with CNS lymphoma. Comparison of predictive value of intraoperative MRI and intraoperative histological examination for diagnostic biopsy yield. *Brain Spine.* (2024) 4:103926. doi: 10.1016/j.bas.2024.103926